Energetics and Kinetics of Interfacial Electron-Transfer Processes at Chemically Modified InP/Liquid Junctions

Nicholas Prokopuk and Nathan S. Lewis*

210 Noyes Laboratory, 127-72, Division of Chemistry and Chemical Engineering, California Institute of Technology, Pasadena, California 91125

Received: October 24, 2002; In Final Form: November 24, 2003

The electrochemical behavior of freshly etched (111)B-oriented InP surfaces was compared to that of (111)B-oriented InP surfaces that had been chemically modified by reaction with *p*-$BrCH_2C_6H_4CF_3$. Differential capacitance versus potential and current density versus potential techniques were used to measure the energetics and kinetics of interfacial electron-transfer reactions in contact with a 70:30 (v:v) mixture of CH_3CN−tetrahydrofuran that contained either 1,1′-dimethylferrrocene$^{+/0}$ or decamethylferrocene$^{+/0}$. For both the etched and modified (111)B InP contacts, plots of differential capacitance versus potential measurements indicated a linear dependence of the equilibrium voltage drop (V_{bi}) in the semiconductor space-charge region, as a function of the redox potential ($E(A/A^-)$) of the solution, with the slope of V_{bi} vs $E(A/A^-) \approx 1.0$, as expected for ideal behavior of a semiconductor/liquid junction. The barrier heights calculated for the chemically modified InP/liquid junctions were 100 ± 20 mV higher than the barrier heights of freshly etched, unmodified (111)B InP surfaces in contact with the same electrolyte solutions. The higher barrier heights of the chemically modified surfaces are consistent with a shift in the InP band-edge energies induced by the surface modification process. The modified and etched surfaces both displayed interfacial electron-transfer kinetics that were first order in the concentration of acceptors in solution and first order in the concentration of electrons at the semiconductor surface. The interfacial electron-transfer rate constants for these systems were determined to be $\sim 10^{-17}-10^{-18}$ cm^4 s^{-1}.

I. Introduction

As electronic devices get smaller and surface area-to-volume ratios consequently become larger, the chemical, electrical, and electronic properties of semiconductor surfaces will become increasingly important in determining the overall device properties. Chemical modification of the electrical properties of semiconductor surfaces is an important step in the formation of molecular electronic devices, photoelectrochemical cells,[1] semiconductor-based chemical sensors,[2,3] and other types of optical and electronic devices.[4] Several methods have recently been developed for modification of silicon surfaces, including chemical reactions of H-terminated silicon with Grignard reagents,[5−7] carboxylic acids,[8] aldehydes,[9,10] alcohols,[7,10−15] alkenes,[5,9,16,17,19−25] and amines.[26] In particular, alkyl termination of silicon has been shown to produce improved chemical, electrochemical, electrical, and sensing properties of such surfaces under a variety of external conditions.[26−31]

By comparison, relatively few strategies have been developed for functionalizing the surfaces of group III−V semiconductors, such as InP and GaAs.[32−36] One goal of surface functionalization is to effect a modification of the chemical properties of the semiconductor surface without producing a significant number of electrical defects at the interface between the semiconductor and the molecular overlayer. Previous work from our laboratory has shown that the reactivity of chemically etched (111)B InP surfaces is consistent with the presence of surficial −OH functionality.[34,35] Consequently, conventional organic reactions such as nucleophilic attack on benzyl bromides can be used in a straightforward fashion to functionalize this phosphorus-rich polar face of the InP lattice. However, no information is yet available on the electrochemical properties of the resulting functionalized (111)B InP surface. In this work, we describe the energetics and kinetics of interfacial electron-transfer reactions of (111)B-oriented InP surfaces that have been modified with covalently attached benzyl functionality. The electrochemical behavior of solid/liquid junctions formed from such electrodes demonstrates that an organic functionality can be covalently attached to InP surfaces without compromising the electrical properties of the semiconductor surface.

II. Experimental Section

A. Materials. The solvents CH_3CN, CH_3OH, and tetrahydrofuran (THF) were dried over CaH_2, Mg/I_2, and Na-benzophenone, respectively, and were then distilled under a gaseous N_2 atmosphere prior to use. The redox couples 1,1′-dimethylferrocene (Me_2Fc) and decamethylferrocene ($Me_{10}Fc$) were obtained from Strem Chemicals or Aldrich Chemical Corporation and were sublimed prior to use. The tetrafluoroborate salts of Me_2Fc^+ and $Me_{10}Fc^+$ were prepared by the method of Hendrickson et al.[37] The $LiClO_4$ electrolyte was fused at 240 °C under vacuum and then was stored under gaseous N_2. *p*-$BrCH_2C_6H_4CF_3$ was obtained from Aldrich Chemical Corporation. All solids were stored in a $N_2(g)$-purged drybox until use.

B. Preparation of Electrodes. Nominally undoped (dopant density of 5.2×10^{15} cm^{-3}), (111)B-oriented, *n*-type InP wafers were obtained from Crysta-Comm, Inc. (Mountain View, CA). Wafers were diced into pieces $\sim 0.1-0.3$ cm^2 in area, and

* Author to whom correspondence should be addressed. E-mail: nslewis@its.caltech.edu.

10.1021/jp0223049 CCC: $27.50
Published on Web 03/16/2004

electrodes were fabricated from these pieces, as described previously.[38] The exposed geometric area of each InP electrode was determined digitally from an enlarged scanned image of the electrode.

Etching and chemical modification of the InP samples was performed in the gaseous N_2 atmosphere of a purge box. Etched InP surfaces were prepared using the following four-step sequence: (a) immersion for 30 s into a solution of 0.05% (v/v) Br_2 in CH_3OH, (b) rinsing with CH_3OH, (c) immersion for 30 s into a solution of 2.0 M NH_3 in CH_3OH, and (d) rinsing with CH_3OH.[39] The complete etching and rinsing sequence was performed two consecutive times for each electrode. Electrodes were then either immediately used in electrochemical experiments or were promptly exposed to a 0.2 M solution of *p*-$BrCH_2C_6H_4CF_3$ in CH_3CN for 2 h at 60 °C, followed by rinsing with CH_3CN and drying under a stream of gaseous N_2.

X-ray photoelectron spectroscopy (XPS) was used to monitor the species on the etched and chemically modified InP surfaces. XPS data were collected with an M-probe spectrometer (VG Instruments) pumped by a CTI Cryogenics-8 cryopump.[35] Surfaces were exposed to monochromatic Al Kα X-rays at a 35° angle of incidence, relative to the surface horizontal. Photoelectrons were collected by a hemispherical analyzer at a takeoff angle of 35° from the sample surface. XPS data were compared with spectra published previously for (111)B InP surfaces that had been modified with *p*-$BrCH_2C_6H_4CF_3$,[35] and chemical modification of the InP surface was deemed satisfactory if the ratio of the F 1s signal to the In $3p_{3/2}$ signal was within 30% of the published value of 0.26.

C. Electrochemistry. Electrochemical cells were prepared inside a $N_2(g)$-purged box. Electrolytes consisted of the desired redox couple dissolved in a solution of 0.5 M $LiClO_4$ in 30% THF−70% CH_3CN (v/v). All electrochemical measurements were performed using a three-electrode cell configuration with a platinum-mesh counter electrode and a platinum wire reference electrode that was poised at the Nernstian potential of the solution. Linear sweep voltammetry measurements were made using a Solartron model 1286 electrochemical analyzer. Impedance measurements were performed using the Solartron electrochemical analyzer in conjunction with a Solartron model 1250 frequency response analyzer. The amplitude of the ac signal was 10 mV and the frequency response was determined between 0.1 Hz and 10^5 Hz. Data were analyzed only when the signals exhibited a phase angle of $>70°$ of the measured current, with respect to the input voltage signal. The electrochemical potential of the solution (E(A/A$^-$)) that was monitored by the platinum reference electrode was measured, with respect to a methanolic saturated calomel electrode (MSCE), before and after each electrochemical experiment, to ensure that the electrolyte composition did not change significantly during the experiment.

Working electrodes consisted of either etched or $F_3CC_6H_4$-CH_2-modified (111)B InP surfaces. After immersion of an electrode into one of the ferrocene-containing electrolytes, current density versus potential ($J-E$) properties were measured, impedance data were collected, a second $J-E$ data set was collected to confirm that no changes had occurred over the time frame of the measurements. Immediately after data collection in one ferrocene-containing solution, the electrode was rinsed with CH_3CN−THF (70:30, v/v), dried under a stream of flowing nitrogen gas, and immersed into the next ferrocene-containing electrolyte, and then further electrochemical data were collected. Chemical etching between electrolytes was avoided, because the electrochemical performance of the InP surfaces was observed to deteriorate after multiple exposures to the etching solutions. Consequently, InP electrodes were used no more than three times (three sets of chemical etches) after receipt from the manufacturer. After the electrochemical measurements were made with the last ferrocene solution, the InP electrode was reimmersed in the first ferrocene solution, to ensure that any changes in the flat band potentials were due to variations in the Nernstian potential of the solution, rather than resulting from the continual exposure to the electrolyte solutions.

D. Determination of Interfacial Rate Constants. Rate constants for interfacial electron-transfer reactions were determined as described previously.[40] In brief, the current density of electron flow from the conduction band of an *n*-type semiconductor to an electron acceptor randomly dissolved in the electrolyte solution is described by

$$J_{et}(E) = -qk_{et}n_s(E)[A] \tag{1}$$

where J_{et} (in units of A cm^{-2}) is the current density due to the charge-transfer process, E (given in volts) the applied potential, q (given in coulombs) the elementary charge, k_{et} (in units of cm^{-4} s^{-1}) the second-order rate constant, n_s (in units of cm^{-3}) the electron concentration at the surface of the semiconductor, and [A] (also in units of cm^{-3}) the concentration of the acceptor species that participates in the electron-transfer process.[41,42] The surface electron concentration is expressed in units of cm^{-3}, because the surface electron concentration varies with the electron concentration in the bulk (n_b) through a Boltzmann factor:

$$n_s(E) = n_b \exp\left[-\frac{q(E + V_{bi})}{kT}\right] \tag{2}$$

where V_{bi} is the built-in voltage of the space-charge region of the semiconductor under conditions of charge-transfer equilibrium with the solution phase.[4] For an *n*-type semiconductor, n_b is equal to the dopant density in the bulk of the semiconductor (N_d).[4] From the rate law of eq 1 and the potential dependence of the surface electron concentration in eq 2, under a forward bias, J_{et} is expected to vary exponentially with E (wth a diode quality factor of 1.0) and linearly with [A].[1,4,43,44] When these criteria are met, the desired electron-transfer rate constant k_{et} can be extracted as long as V_{bi} is known for the system of interest.[41,42,45]

The built-in voltage for each *n*-InP/liquid junction of interest was calculated from an analysis of the electrochemical impedance data.[42] The impedance data were collected under reverse-bias conditions to minimize contributions of faradaic current flow to the electrochemical response. This constraint greatly simplifies the equivalent circuit to consist of the space-charge resistance (R_{sc}) in parallel with the space-charge capacitance (C_{sc}), both of which are placed in series with the solution resistance (R_s).[42] The contribution of the double-layer capacitance (C_{dl}) on the liquid side of the interface was neglected because this series capacitance is much larger than that of the space-charge region.[42] The built-in voltage was extracted from the potential-dependent impedance data through use of the Mott−Schottky expression:

$$C^{-2} = \frac{2}{q\epsilon\epsilon_0 N_d A_s^2}\left(E + V_{bi} - \frac{kT}{q}\right) \tag{3}$$

where ϵ_0 is the permittivity of free space, ϵ the dielectric constant of the semiconductor, k the Boltzmann constant, T the absolute temperature, and A_s the area of the semiconductor electrode.[42] The absence of a frequency dependence of the measured

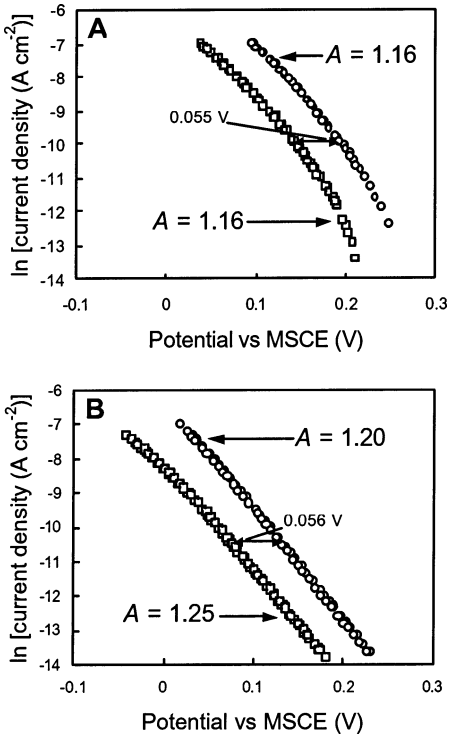

Figure 1. Current density−potential data for (A) *n*-type InP/CH_3CN−THF−$Me_2Fc^{0/+}$ and (B) *n*-type InP−$CH_2C_6H_4CF_3$/CH_3CN−THF−$Me_2Fc^{0/+}$ contacts. Electrolytes are 0.5 M $LiClO_4$ in 30% THF−70% CH_3CN (v/v). 1,1′-Dimethylferrocene concentrations are 0.010 M, and 1,1′-dimethylferrocenium concentrations are 0.100 M (circles) or 0.010 M (squares). Diode quality factors (*A*) were obtained from linear fits of the data to eq 4.

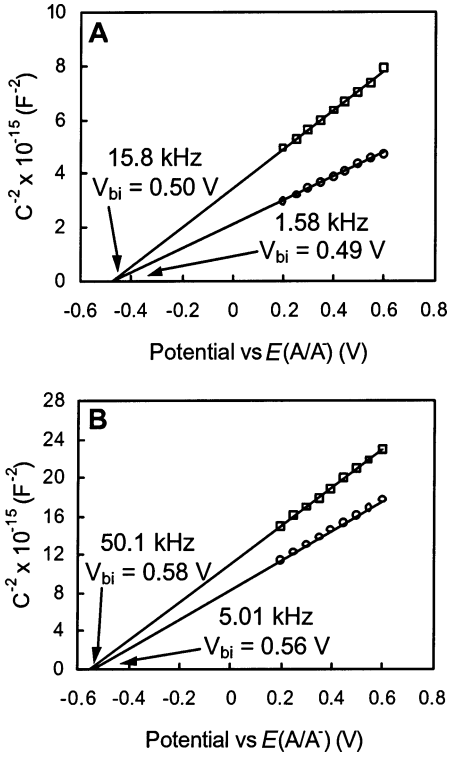

Figure 2. Mott−Schottky plots of C^{-2} vs *E* for (A) *n*-type InP/CH_3-CN−THF−$Me_2Fc^{0/+}$ and (B) *n*-type InP−$CH_2C_6H_4CF_3$/CH_3CN−THF−$Me_2Fc^{0/+}$ contacts. In both cases, the 1,1′-dimethylferrocene concentrations are 0.010 M and the 1,1′-dimethylferrocenium concentrations are 0.010 M. Data are shown for two different frequencies, spanning 1 order of magnitude. Built-in voltages that were obtained by extrapolating to the *x*-intercept are listed for each frequency. Average dopant densities extracted from the slope of the lines are (A) 7.3×10^{15} cm^{-3} and (B) 6.3×10^{15} cm^{-3}.

capacitance, in conjunction with agreement between the observed slope of a plot of C^{-2} vs *E* and the slope predicted from the dopant density of the crystal, as specified by the manufacturer, verified the applicability of the equivalent circuit analysis to the impedance data of interest.

Currents were corrected for concentration overpotentials and solution resistance using methods that have been described previously.[40,46] Current densities (J_{et}) used to determine k_{et} values were at least 1×10^{-4} A cm^{-2} in magnitude, to minimize errors that occur from the presence of alternative recombination pathways (vide infra). Surface electron concentrations were calculated from eq 2 for the same applied potential *E* that was used to obtain the current density. Built-in voltages used to evaluate n_s were those determined for that specific solid/liquid contact. Interfacial electron-transfer rate constants (k_{et}) were then obtained using eq 1 with the calculated n_s values and the measured current densities.

III. Results

A. Rate Constant Measurements for *n*-InP/CH_3CN−THF−1,1′-$Me_2Fc^{+/0}$ Junctions. Figure 1 displays the *J*−*E* behavior of etched and $F_3CC_6H_4CH_2$-modified *n*-InP electrodes in contact with CH_3CN−THF−0.5 M $LiClO_4$−0.010 M Me_2-Fc solutions that contained either 0.100 or 0.010 M of Me_2-Fc^+. Under forward bias ($-E \gg kT/q$), in both cases, the current-density-versus-potential data are well-described by the relationship

$$\ln(-J) = \ln(J_0) - \frac{qE}{AkT} \qquad (4)$$

where *A* is the diode quality factor and J_0 is the exchange current density of the semiconductor/liquid contact.[40] All the semiconductor/liquid contacts studied in this work exhibited diode quality factors of 1.0−1.25. The relatively small deviation from the ideal value of $A = 1.0$ may result from the presence of other transport or loss mechanisms that contribute to the overall current density at increasing forward-bias voltages. However, the observed values of *A* are in good agreement with the expected first-order dependence of the current density on the concentration of electrons at the surface of the semiconductor. In addition, the near-ideal values of *A* indicate that the band-edge position remains fixed in the potential region of interest.

For the etched InP surface, a change in the acceptor concentration from $[Me_2Fc^+] = 0.010$ M to $[Me_2Fc^+] = 0.100$ M resulted in a shift of 55 mV in the current densities along the abscissa of the plot of ln *J* vs *E*. A very similar shift (of 56 mV) was observed for the chemically modified InP surface. These values are similar to the ideal value of 59 mV that is predicted from the second-order rate expression of eq 1.[47] Therefore, the data indicate that the interfaces under study exhibited a first-order dependence of the current density on the acceptor concentration, over the range of acceptor concentrations investigated in this work.

Figure 2 shows the C^{-2} vs *E* data for etched and $CF_3C_6H_4$-CH_2-modified InP electrodes in contact with CH_3CN−THF−0.5 M $LiClO_4$−1,1′-$Me_2Fc^{+/0}$ contacts. Data are shown for $[Me_2Fc] = 0.010$ M and $[Me_2Fc^+] = 0.010$ M. In both panels A and B of Figure 2, the differential capacitance values exhibited some dependence on the input voltage frequency; however, the slopes of the lines of C^{-2} vs *E* yielded values of N_d that were within 50% of the value specified by the manufacturer of the crystal. The data used for analysis were primarily those from

TABLE 1: Interfacial Electron-Transfer Rate Constants for *n*-type InP/Liquid and *n*-type InP−$CH_2C_6H_4CF_3$/Liquid Contacts[a]

concentration of acceptor species, [A] (M)	built-in voltage, V_{bi} (V)[b]	surface electron concentration, n_s (cm^{-3})[c]	current density, J (mA cm^{-2})[d]	interfacial electron-transfer rate constant, k_{et} (cm^4 s^{-1})[e]
		InP/1,1′-Me_2Fc^+		
0.1	0.538 ± 0.012	(4.1 ± 3.5) × 10^{11}	0.212	(5.4 ± 4.7) × 10^{-17}
0.1	0.521 ± 0.008	(3.2 ± 1.9) × 10^{11}	0.259	(8.3 ± 5.0) × 10^{-17}
0.01	0.482 ± 0.005	(3.0 ± 1.2) × 10^{12}	0.190	(6.5 ± 2.6) × 10^{-17}
0.01	0.493 ± 0.007	(1.5 ± 0.8) × 10^{12}	0.250	(1.8 ± 0.9) × 10^{-16}
Average[f]				(7.6 ± 5.2) × 10^{-17}
		InP−$CH_2C_6H_4CF_3$/1,1′Me_2Fc^+		
0.1	0.605 ± 0.009	(4.2 ± 2.4) × 10^{13}	0.725	(1.8 ± 1.0) × 10^{-18}
0.1	0.620 ± 0.005	(1.1 ± 0.3) × 10^{13}	0.167	(1.6 ± 0.5) × 10^{-18}
0.01	0.580 ± 0.008	(8.8 ± 4.7) × 10^{13}	0.194	(2.3 ± 1.2) × 10^{-18}
0.01	0.567 ± 0.008	(7.5 ± 4.1) × 10^{13}	0.577	(8.0 ± 4.4) × 10^{-18}
Average[f]				(4.8 ± 3.2) × 10^{-18}
		InP/$Me_{10}Fc^+$		
0.070	0.200 ± 0.004	(4.4 ± 3.4) × 10^{13}	0.801	(2.7 ± 2.1) × 10^{-18}
0.070	0.233 ± 0.012	(1.5 ± 3.0) × 10^{13}	0.661	(6.6 ± 13.2) × 10^{-18}
0.0070	0.142 ± 0.008	(1.6 ± 3.5) × 10^{14}	0.393	(3.7 ± 8.1) × 10^{-18}
0.0070	0.160 ± 0.008	(2.4 ± 4.7) × 10^{14}	0.745	(4.6 ± 8.9) × 10^{-18}
Average[f]				(7.0 ± 4.5) × 10^{-18}
		InP−$CH_2C_6H_4CF_3$/$Me_{10}Fc^+$		
0.070	0.289 ± 0.011	(1.2 ± 1.7) × 10^{13}	0.260	(3.3 ± 4.9) × 10^{-18}
0.070	0.332 ± 0.007	(4.4 ± 3.6) × 10^{13}	0.322	(1.1 ± 0.9) × 10^{-18}
0.0070	0.221 ± 0.009	(5.3 ± 8.4) × 10^{13}	0.210	(5.9 ± 9.4) × 10^{-18}
0.0070	0.263 ± 0.002	(9.1 ± 2.7) × 10^{13}	0.245	(4.0 ± 1.2) × 10^{-18}
Average[f]				(3.2 ± 3.3) × 10^{-18}

[a] Solutions consisted of 0.1 M $LiClO_4$ in CH_3CN/THF (70:30, v/v); all experiments with 1,1′-$Me_2Fc^{+/0}$ had [A^-] = 0.010 M, and all experiments with $Me_{10}Fc^{+/0}$ had [A^-] = 0.0070 M. [b] Each row reports data for a separate electrode/electrolyte contact, with means and errors for the quantities in each row representing the values obtained from a statistical analysis of the V_{bi} values determined from C^{-2}−E plots at ≥10 different input ac frequencies on that electrode/electrolyte contact. [c] The errors listed are calculated from the propagation of error in V_{bi}. [d] Value shown is the current density at which the rate constant calculation was performed; the calculated rate constant differed slightly at different current densities, because of the value of the diode quality factor (A) deviation slightly from unity. [e] Errors are those due to the uncertainty in n_s for each electrode/electrolyte contact. [f] Mean values of rate constants determined for at least 10 separate electrode/electrolyte contacts, each using different InP electrodes. Errors denote the standard deviation in the rate constants calculated from all of these measurements. Values given in bold represent average values.

the higher-frequency signals, because the use of a higher frequency reduces any residual contribution of capacitance that results from surface-state charging to the measured capacitance of the electrode. Extrapolation of the C^{-2} vs E plots to C^{-2} = 0 yielded V_{bi} values that were constant to within ±15 mV for the different measurement frequencies used in this work. V_{bi} values were calculated from the x-intercepts to be 0.49 and 0.57 V for the etched and $CF_3C_6H_4CH_2$-modified InP electrodes, respectively.

Use of the value for V_{bi}, in conjunction with the data of Figure 1 and the rate law of eq 1, yielded an electron-transfer rate constant of 6.5 × 10^{-17} cm^4 s^{-1} for this specific etched n-InP electrode at [Me_2Fc^+] = 0.010 M. The n-InP electrode that had been modified with $BrCH_2C_6H_4CF_3$ yielded k_{et} = 8.0 × 10^{-18} cm^4 s^{-1} at [Me_2Fc^+]= 0.010 M. The calculated value of k_{et} did not change, within experimental error, when the concentration of oxidized species was varied, in accord with expectations based on a second-order rate law and lack of Fermi level pinning of the InP/liquid contacts in the potential range investigated. For at least 10 electrodes of each type in contact with $Me_2Fc^{+/0}$ solutions, average values of k_{et} = (7.6 ± 5.2) × 10^{-17} cm^4 s^{-1} were observed for etched electrodes and average values of k_{et} = (4.8 ± 3.2) × 10^{-18} cm^4 s^{-1} were observed for $F_3CC_6H_4$-CH_2-modified InP electrodes (Table 1).

B. Rate Constant Measurements for *n*-InP and *n*-InP−$CH_2C_6H_4CF_3$/CH_3CN−THF−$Me_{10}Fc^{+/0}$ Junctions. Analogous experiments were performed for n-InP/CH_3CN−THF−0.5 M $LiClO_4$ $Me_{10}Fc^{+/0}$ contacts. Figure 3 shows the J−E response of etched and $F_3CC_6H_4CH_2$-modified InP electrodes in contact with solutions that had [$Me_{10}Fc$] = 0.0070 M and [$Me_{10}Fc^+$] values of either 0.070 or 0.0070 M. The data were qualitatively similar to those obtained for InP/$Me_2Fc^{0/+}$ contacts in that diode quality factors were 1.00−1.25, indicating ideal behavior and a first-order dependence of the electron-transfer rate on the concentration of electrons at the semiconductor surface. In addition, the separation between the J−E data for both the etched and modified InP electrodes at the two different $Me_{10}Fc^+$ concentrations was very similar to the theoretically expected value of 59 mV. Thus, the reaction kinetics were first order in regard to the concentration of electrons at the semiconductor surface and first order in regard to the concentration of acceptors in solution, as predicted by eq 1.

Figure 4 displays the C^{-2}−E plots for these InP samples in contact with CH_3CN−THF − 0.0070 M $Me_{10}Fc$−0.0070 M $Me_{10}Fc^+$ solutions. Qualitatively, the differential capacitance behavior closely resembled that observed for InP/CH_3CN−THF−1,1′-$Me_2Fc^{0/+}$ contacts. A measurable frequency dispersion was observed for the InP/CH_3CN−THF−$Me_{10}Fc^{+/0}$ contacts; however, the built-in voltages calculated from the impedance analysis varied only slightly (±15 mV) as the frequency of the applied voltage was varied. Furthermore, the dopant densities calculated from the slopes of C^{-2}−E plots of such junctions were in good agreement with the values provided by the manufacturer of the crystals. Electron-transfer rate constants for the junctions in Figure 3 at [$Me_{10}Fc^+$] = 0.0070 M were determined to be 4.6 × 10^{-18} cm^4 s^{-1} for etched n-InP and 7.4 × 10^{-18} cm^4 s^{-1} for n-InP−$CH_2C_6H_4CF_3$ electrodes, and average rate constants for ≥10 electrodes of each type in contact with the $Me_{10}Fc^{+/0}$ electrolyte solutions were k_{et} = (7.0 ± 4.5) × 10^{-18} cm^4 s^{-1} for etched surfaces and k_{et} = (3.2 ± 3.3) × 10^{-18} cm^4 s^{-1} for $F_3CC_6H_4CH_2$-modified n-InP surfaces (Table 1).

The slight nonideality of the J−E behavior (A > 1) implies that the calculated k_{et} values will vary slightly with the current

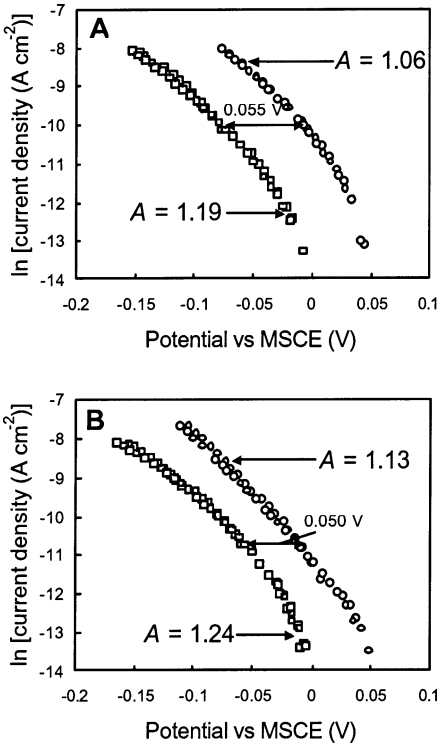

Figure 3. Current density−potential data for (A) *n*-type InP/CH_3CN−THF−$Me_{10}Fc^{0/+}$ and (B) InP−$CH_2C_6H_4CF_3$/CH_3CN−THF−$Me_{10}Fc^{0/+}$ contacts. Electrolytes are 0.5 M $LiClO_4$ in 30% THF−70% CH_3OH (v/v). Decamethylferrocene concentrations are 0.0070 M, and decamethylferrocenium concentrations are 0.070 M (circles) or 0.0070 M (squares). Diode quality factors (*A*) were obtained from linear fits of the data to eq 4.

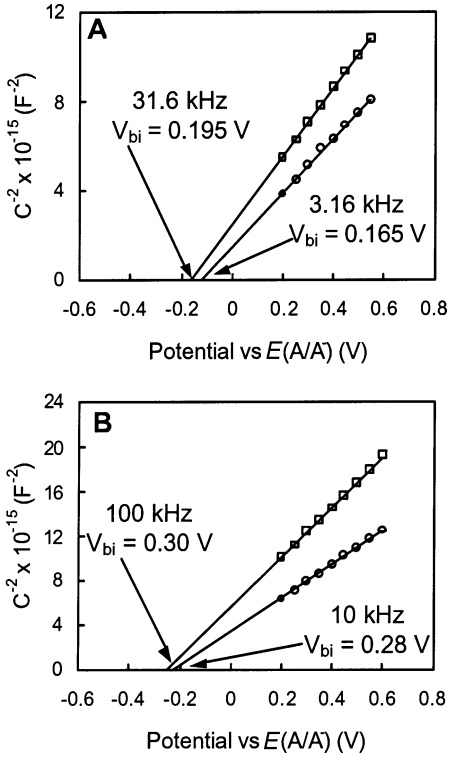

Figure 4. Mott−Schottky plots for (A) *n*-type InP/CH_3CN−THF−$Me_{10}Fc^{0/+}$ and (B) *n*-type InP−$CH_2C_6H_4CF_3$/CH_3CN−THF−$Me_{10}Fc^{0/+}$ contacts. In both cases, the decamethylferrocene concentrations are 0.0070 M and the decamethylferrocenium concentrations are 0.0070 M. Data are shown for two different frequencies, spanning 1 order of magnitude. Built-in voltages were obtained by extrapolating to the *x*-intercept and are listed for each frequency. Average dopant densities extracted from the slope of the lines are (A) 4.9×10^{15} cm^{-3} and (B) 3.0×10^{15} cm^{-3}.

density used in the calculation. For example, the diode quality factor of 1.19 for the $J-E$ curve in Figure 3A with [$Me_{10}Fc^+$] of 0.0070 M leads to a calculated value of $k_{et} = 2.3 \times 10^{-18}$ $cm^4\ s^{-1}$ for $J = -1.78 \times 10^{-4}$ A cm^{-2} and a value of $k_{et} = 4.1 \times 10^{-18}$ $cm^4\ s^{-1}$ for $J = -6.54 \times 10^{-6}$ A cm^{-2}. Most alternative recombination processes (surface state or depletion region recombination pathways) exhibit larger values of *A*; therefore, the second-order rate process that has the lowest value of *A* will dominate the total current at larger current densities. Thus, current densities measured at increasingly negative forward bias are more likely to provide rate constants closer to the true value, and these values are the ones tabulated in Table 1.

IV. Discussion

Semiconductor/liquid junctions constructed from (111)B *n*-InP surfaces modified with *p*-$BrCH_2C_6H_4CF_3$ displayed almost-ideal energetic and interfacial charge-transfer kinetics behavior when contacted with the ferrocene-based redox couples that have been investigated in this work. Specifically, the interfacial charge-transfer kinetics of etched and $CF_3C_6H_4CH_2$-modified InP/liquid contacts were in accord with the second-order rate expression expected for a simple electron-transfer event from a delocalized electron in the conduction band of a semiconductor to an outer-sphere, one-electron redox acceptor species dissolved in an electrolyte solution. In contrast, Si(111) surfaces alkylated with olefins through a radical addition process have been found to exhibit highly nonideal diode quality factors of ~4 and negligible current density until potentials far negative of the flat-band potential (i.e., sufficient to drive the semiconductor into an accumulation condition) were applied.[48] In addition, the InP $C^{-2}-E$ data indicate that the band-edge positions for both chemically modified InP and freshly etched InP electrode surfaces remained constant when in contact with electrolytes that spanned a significant range of electrochemical potentials, again in accord with behavior expected for an ideally behaving semiconductor/liquid contact.

SCHEME 1

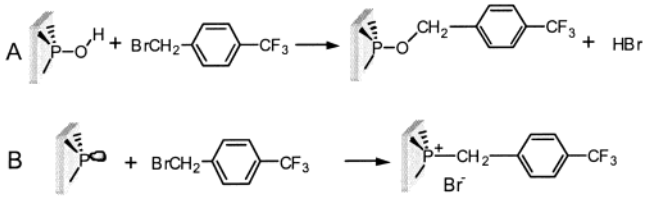

A. Chemical Modification of (111)B InP with $BrCH_2C_6H_4CF_3$. The chemical modification of (111)B *n*-InP with $BrCH_2C_6H_4CF_3$ used a procedure published previously in which the putative −OH functionality on anaerobically etched (111)B *n*-InP surfaces reacts with the alkly halide to produce a covalent linkage between the semiconductor and the organic benzyl group (see Scheme 1A).[34,35] Successful modification of the *n*-InP surface was deduced from the presence of an intense F 1s signal in the XPS spectrum as well from the appearance of a smaller C_F signal arising from the fluorinated $-CF_3$ carbon atom on the functionalization reagent.[35] Chemically modified InP samples that were used for electrochemical measurements were not subject to routine XPS analysis. However, InP samples were periodically examined with XPS and the measured spectra were compared to published XP spectra of (111)B InP surfaces that had been modified $BrCH_2C_6H_4CF_3$. Successful chemical modi-

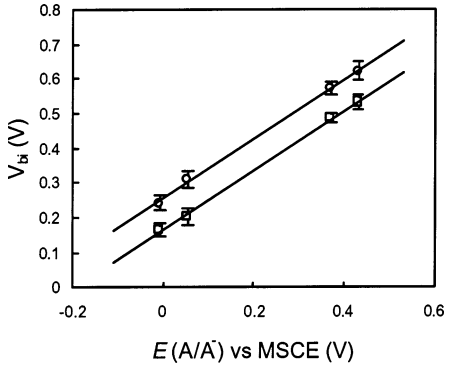

Figure 5. Dependence of the built-in voltage (V_{bi}) of (□) *n*-InP and (○) *n*-InP−$CH_2C_6H_4CF_3$ electrodes on the Nernstian potential (E(A/A$^-$)) of solution contacts with the one-electron, outer-sphere redox systems 1,1′-dimethylferrocene$^{0/+}$ and decamethylferrocene$^{0/+}$. Nernstian potentials have been referenced with respect to a methanolic SCE. The mean V_{bi} value of every electrode/electrolyte contact was determined using at least 10 ac input voltage frequencies, and the means and standard deviations of these mean V_{bi} values for at least five separate electrodes are depicted at each value of E(A/A$^-$). Linear regression for the two sets of data yields slopes of 0.85 and 0.86 for the etched and $BrCH_2C_6H_4CF_3$-modified InP, respectively.

fication of the (111)B InP was determined by comparing the ratio of the F 1s and In $3p_{3/2}$ signals with published values.[35] The success rate for chemical modification with $BrCH_2C_6H_4CF_3$ was found to be >90%.

B. Energetic Properties of *n*-InP/Liquid and *n*-InP−$CH_2C_6H_4CF_3$/Liquid Junctions. The ideal energetic behavior reported for freshly etched *n*-InP/CH_3CN−THF junctions and for chemically modified InP−$CH_2C_6H_4CF_3$/CH_3CN−THF junctions is similar to the behavior observed previously by Koval et al.[49] for *n*-InP/CH_3CN contacts as well as that observed by Pomykal et al.[47] for *n*-InP/CH_3OH and *n*-InP/CH_3OH−THF junctions. In these systems, the band-edge positions remain unchanged when the semiconductor is placed in contact with electrolytes that have significantly different Nernstian redox potentials.

Figure 5 displays the built-in voltages of a series of *n*-InP/CH_3CN−THF and InP−$CH_2C_6H_4CF_3$/CH_3CN−THF contacts as a function of the redox potential of the electrolyte, as deduced from the differential-capacitance-versus-potential behavior of these interfaces. For both types of electrodes, the V_{bi}−E(A/A$^-$) plots are well-fitted by a straight line with a slope of 0.86 for the etched surface and 0.85 for the modified (111)B InP surface. Thus, the energetics of these series of contacts exhibit almost-ideal behavior over this potential range.

In semiconductor/liquid contacts that do not display significant Fermi level pinning, changes in the Nernstian redox potential of the solution should result in the same magnitude of change in the built-in voltage of the semiconductor/liquid contact. Hence, in such systems, the equilibrium band bending is not determined primarily by surface states but rather by the thermodynamic properties of the electrolyte. This observation is especially significant for the modified InP surfaces, because it indicates that the covalent attachment of a benzyl group to the (111)B InP surface occurs without introducing significant amounts of surface states that might compromise the electrochemical properties of the InP. An upper limit on the number of surface states at such contacts can be estimated from the V_{bi}−E(A/A$^-$) plots. With an estimated Helmholtz layer capacitance of 10 μF cm^{-2} and a double-layer thickness of 3 Å, surface state densities of 10^{12} cm^{-2} (N_{ss}) would suffice to pin the Fermi level of the semiconductor surface.[50] Within this context, the

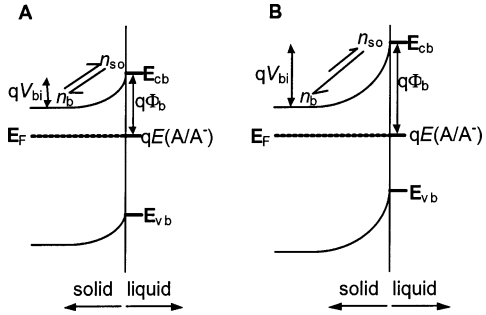

Figure 6. Energy diagram for (A) etched and (B) $CF_3C_6H_4CH_2$-modified *n*-type InP. $\mathbf{E}_{cb}$ and $\mathbf{E}_{vb}$ are the conduction-band- and valence-band-edge energies at the surface of the semiconductor, respectively; V_{bi} is the built-in voltage of the semiconductor/liquid contact, and ϕ_b is the barrier height. At equilibrium, the surface electron concentration (n_s) is related to the electron concentration in the bulk of the semiconductor by a Boltzmann factor. When the InP surface is chemically modified with $BrCH_2C_6H_4CF_3$, the band-edge positions are shifted closer to the vacuum level, resulting in a larger built-in voltage and a lower surface electron concentration in contact with the same electrolyte solution.

linearity of the data in Figure 5 implies an upper limit of N_{ss} < 10^{11} cm^{-2} for the InP−$CH_2C_6H_4CF_3$/liquid junctions. With a surficial atomic density of 10^{15} atoms cm^{-2} and an electrically active effective defect density of <10^{11} cm^{-2}, no more than one atomic site per 10^4 surface atoms can act as an effective electrical trap site on benzyl-modified InP surfaces. Consistently, time-resolved photoluminescence measurements on $CF_3C_6H_4CH_2$-modified (111)B InP surfaces indicate surface recombination velocities of 100 cm s^{-1} for such systems, which suggests an even lower limit of one defect per 10^5 surface atoms on such modified surfaces in contact with air ambients.[35] Taken together, the photoluminescence studies and the C^{-2}−E measurements provide an internally consistent picture regarding the electrical properties of benzylated (111)B InP surfaces.

The data of Figure 5 also indicate that the built-in voltages obtained for the $CF_3C_6H_4CH_2$-modified InP surface are 100 ± 20 mV larger than those obtained for etched *n*-InP in contact with the identical electrolyte solutions. Hence, the band edges are shifted to more-negative potentials by 100 ± 20 mV for $CF_3C_6H_4CH_2$-modified surfaces, as compared to etched *n*-InP surfaces (see Figure 6). The shift of the band-edge energy for the modified surface can be rationalized in terms of the chemistry of the functionalization process, which should effect replacement of the hydroxyl proton of (111)B InP by a more electron-donating benzyl group (see Scheme 1A). This change in the surface-attached functionality is expected to increase the electron density at the InP surface, thereby increasing the potential energy of electrons at the benzyl-modified surface, relative to the potential energy of electrons at the etched InP surface. Notably, the observed negative shift in the band-edge energy is not in accord with expectations for a surface functionalization process in which the chemistry of the etched phosphorus-rich (111)B InP face is dominated by lone pairs on the surface P atoms (see Scheme 1B).[51] Such a reactivity pathway would yield a layer of phosphonium cations immediately adjacent to the semiconductor surface, with the introduction of additional positive charge at the InP surface being expected to produce a shift in the band energies of functionalized surfaces to more-positive potentials, relative to that of the unmodified (111)B InP surface.

The shift in band edges that results from the surface modification process is additionally significant, because it demonstrates that the energetics of a semiconductor interface

can be controlled through molecular manipulations at the surface.[52−55] In contrast to the shifting of the band edges of metal oxide semiconductors through changing the pH of the solution,[56−59] the band-edge shift of the InP with the benzyl modification process is independent of the redox potential of the solution. The covalent nature of the interaction and the electronic properties of the molecule are likely the dominating factor in determining the magnitude of the band shifts, which suggests that the functionalization method can provide rational, molecular-level control over the work function (or, equivalently, control over the magnitude of the surface dipole layer induced by the surface modification process) and other electrical properties of (111)B InP surfaces.

C. Comparison between the Interfacial Electron-Transfer Kinetics at *n*-InP/Liquid and *n*-InP−$CH_2C_6H_4CF_3$/Liquid Contacts. The etched and $CF_3C_6H_4CH_2$-modified InP surfaces both exhibited ideal interfacial charge-transfer kinetics behavior in contact with the ferrocene-containing electrolytes, allowing for direct measurement of the interfacial rate constants with a system that has a molecular layer directly attached to the semiconductor surface. To our knowledge, such ideal interfacial kinetics behavior for a series of redox couples has been reported previously only for *n*-type Si/CH_3OH and *n*-type InP/CH_3OH junctions.[40,47,60]

The rate constants obtained for the etched and modified *n*-InP/liquid junctions (see Table 1) are generally consistent with theoretical expectations. A series of semiclassical Marcus theory treatments and, in addition, a Fermi Golden Rule-based formalism all yield estimates of the maximum rate constant value of $k_{et,max} \approx 10^{-17}$ cm^4 s^{-1} for interfacial electron-transfer reactions from the conduction band of an *n*-type semiconductor to a one-electron, outer-sphere, nonadsorbing redox couple dissolved in the electrolyte solution.[38,41,45,61] Consistently, silicon/liquid and InP/liquid contacts that have been studied previously in our laboratory were observed to exhibit interfacial electron-transfer rate constants in the range of 10^{-16}−10^{-18} cm^4 s^{-1}.[40,47,60] In addition, scanning electrochemical microscopy techniques on the *p*-$WSe_2/H_2O-Ru(NH_3)_6^{3+/2+}$ interface have yielded k_{et} values of 5.7×10^{-17} cm^4 s^{-1}.[62]

The addition of the benzyl layer to the InP/liquid junction adds an organic barrier that separates electrons in the conduction band and acceptors in solution and, in addition, shifts the band edges of the InP. Hence, both the charge-transfer distance and the driving force are changed by the surface modification process. The effect of an organic spacer on intramolecular and interfacial electron-transfer rate constants at metal electrodes is well understood, and the rate constant should vary with the chemical nature and length of the organic bridge. Adaptation of the Marcus formalism for electron transfer at a liquid/liquid interface to the situation for a semiconductor interface in which delocalized electrons in the conduction band of the semiconductor combine with an acceptor species dissolved in solution produces the following relation:

$$k_{et} = \nu_n \kappa_{et} \kappa_n \tag{5}$$

where the attempt frequency (ν_n) describes the relevant nuclear vibrational terms and is $\sim 10^{13}$ s^{-1}.[41,63] The nuclear factor (κ_n) is given by

$$k_{et} = \exp\left[-\frac{(\lambda + \Delta G^{\circ\prime})^2}{4\lambda kT}\right] \tag{6}$$

where λ is the total reorganization energy of the acceptor in solution and $\Delta G^{\circ\prime}$ is the standard free energy of reaction for the electron transfer. The distance dependence of the electronic coupling term (κ_{el}) is assumed to be

$$\kappa_{el} = \kappa_{el,o} \exp[-\beta(R - r_e - r_a)] \tag{7}$$

where $\kappa_{el,0}$ is the electronic term at the closest approach of the reactants, R is the distance between the electron in the conduction band and the acceptor in solution, and r_e and r_a are the effective radii of the acceptor in solution and of the electron in the solid, respectively. The electronic coupling decay constant (β) has been determined experimentally for a variety of chemical species, and values of $\beta \approx 1$ Å^{-1} have been found for methylene spacers whereas $\beta \approx 0.2$ Å^{-1} for conjugated spacers.[64−66]

The decrease in the electronic coupling term for InP modified by $BrCH_2C_6H_4CF_3$ can be estimated through the use of the reported values of β for methylene and phenyl groups. Although β values have not been reported for electron tunneling though $-CF_3$ groups, a reasonable estimate of 1 Å^{-1} can be used. Given these values, the value of κ_{el} for InP−$CH_2C_6H_4CF_3$/liquid junctions is expected to be 1.5 orders of magnitude lower than κ_{el} for etched InP/liquid contacts. This calculation assumes that the surface coverage of benzyl groups is uniform and that the overlayer is composed of benzyl moieties oriented normal to the surface plane[33] without a significant number of pinholes that would facilitate electron transfer at smaller InP−electron acceptor distances; hence, it is an upper limit for the expected variation in the experimentally determined rate constant change upon surface modification. Inspection of the rate constants for the etched and modified InP indicates that the interfacial electron-transfer process for the modified InP surface is somewhat attenuated, compared to that for the etched InP. The differences in the k_{et} values are within the error bars of the measurements, with the exception of the calculated value for etched *n*-InP/$CH_3CN-THF-Me_2Fc^{+/0}$ junctions, which is significantly higher than that for the modified surface or the *n*-InP/$CH_3CN-THF-Me_{10}Fc^{+/0}$ junctions. Fewer methyl groups on 1,1′-Me_2Fc^+ and the absence of the benzyl film likely contribute to increased κ_{el} and k_{et} values. Note that the shifting of the band edges will also affect k_{et} slightly, through adjustment of the standard free-energy change $\Delta G^{\circ\prime}$ and the nuclear term κ_n. However, a change of only 0.1 eV in $\Delta G^{\circ\prime}$ is not expected to measurably affect κ_n or k_{et}. For example, a λ value of 0.8 eV for 1,1′-Me_2Fc and a change in $\Delta G^{\circ\prime}$ from −0.6 eV to −0.7 eV results in a change in κ_n from 0.62 to 0.87.[67] Similarly, the local dielectric constant near a methyl-terminated electrode could be somewhat smaller than that near a polar electrode surface, producing a decrease in λ that might also affect k_{et} for the systems of interest. Additional measurements with longer-chain-length functional groups are needed to fully elucidate the value of the attenuation coefficient in such systems; however, the ideal energetics and charge-transfer kinetics behavior exhibited upon surface modification suggests that such an approach will be especially fruitful using the modification routes of (111)B InP surfaces described herein.

V. Conclusions

The *n*-type InP/liquid and *n*-type InP−$CH_2C_6H_4CF_3$/liquid contacts investigated in this work demonstrated almost-ideal energetic and kinetics behavior. Rate constants for interfacial electron-transfer processes with ferrocenium redox couples dissolved in solution were obtained, and the observed values were consistent with those measured for other semiconductor/liquid contacts. The effect of the $BrCH_2C_6H_4CF_3$-modification process is most evident in the shifting of the band edges of the

InP. Band-edge energies at $CF_3C_6H_4CH_2$-modified surfaces are 100 ± 20 mV more negative than those for etched InP. The shift to lower energies upon reaction with $BrCH_2C_6H_4CF_3$ is consistent with the surface chemistry of (111)B InP being dominated by surfacial hydroxyl groups rather than electron lone pairs on the P atom undergoing an alkylation reaction. The ideal energetic behavior displayed by the $CF_3C_6H_4CH_2$-modified InP/liquid contacts indicates that the chemical modification process does not introduce significant levels of electrical defects at the surface. Thus, applications of this surface chemistry in semiconductor technology will not be limited by the electrical quality of the prepared surfaces. In fact, the ideal kinetics and energetics demonstrated by the $CF_3C_6H_4CH_2$-modified InP/liquid contacts suggest that this chemistry is well-suited for constructing devices with controlled and predictable electrical properties.

Acknowledgment. We acknowledge the Department of Energy, Office of Basic Energy Sciences, for support of this work.

References and Notes

(1) Fonash, S. J. *Solar Cell Device Physics*; Academic: New York, 1981.
(2) Moore, D. E.; Lisensky, G. C.; Ellis, A. B. *J. Am. Chem. Soc.* **1994**, *116*, 9487−9491.
(3) Sze, S. M. *Semiconductor Sensors*; Wiley: New York, 1994.
(4) Sze, S. M. *Physics of Semiconductor Devices*, 2nd ed.; Wiley: New York, 1981.
(5) Boukherroub, R.; Morin, S.; Bensebaa, F.; Wayner, D. D. M. *Langmuir* **1999**, *15*, 3831−3835.
(6) Yu, H. Z.; Boukherroub, R.; Morin, S.; Wayner, D. D. M. *Electrochem. Commun.* **2000**, *2*, 562−566.
(7) Mitchell, S. A.; Boukherroub, R.; Anderson, S. *J. Phys. Chem. B* **2000**, *104*, 7668−7676.
(8) Lee, E. J.; Bitner, T. W.; Ha, J. S.; Shane, M. J.; Sailor, M. J. *J. Am. Chem. Soc.* **1996**, *118*, 5375−5382.
(9) Effenberger, F.; Gotz, G.; Bidlingmaier, B.; Wezstein, M. *Angew. Chem., Int. Ed. Engl.* **1998**, *37*, 2462−2464.
(10) Boukherroub, R.; Morin, S.; Sharpe, P.; Wayner, D. D. M.; Allongue, P. *Langmuir* **2000**, *16*, 7429−7434.
(11) Haber, J. A.; Lauermann, I.; Michalak, D.; Vaid, T. P.; Lewis, N. S. *J. Phys. Chem. B* **2000**, *104*, 9947−9950.
(12) Kim, N. Y.; Laibinis, P. E. *J. Am. Chem. Soc.* **1997**, *119*, 2297−2298.
(13) Cleland, G.; Horrocks, B. R.; Houlton, A. *J. Chem. Soc., Faraday Trans.* **1995**, *91*, 4001−4003.
(14) Eagling, R. D.; Bateman, J. E.; Goodwin, N. J.; Henderson, W.; Horrocks, B. R.; Houlton, A. *J. Chem. Soc., Dalton Trans.* **1998**, 1273−1275.
(15) Bateman, J. E.; Eagling, R. D.; Horrocks, B. R.; Houlton, A. *J. Phys. Chem. B* **2000**, *104*, 5557−5565.
(16) Terry, J.; Mo, R.; Wigren, C.; Cao, R. Y.; Mount, G.; Pianetta, P.; Linford, M. R.; Chidsey, C. E. D. *Nucl. Instrum. Methods Phys. Res., Sect. B* **1997**, *133*, 94−101.
(17) Terry, J.; Linford, M. R.; Wigren, C.; Cao, R. Y.; Pianetta, P.; Chidsey, C. E. D. *Appl. Phys. Lett.* **1997**, *71*, 1056−1058.
(18) Terry, J.; Linford, M. R.; Wigren, C.; Cao, R. Y.; Pianetta, P.; Chidsey, C. E. D. *J. Appl. Phys.* **1999**, *85*, 213−221.
(19) Boukherroub, R.; Wayner, D. D. M. *J. Am. Chem. Soc.* **1999**, *121*, 11513−11515.
(20) Cicero, R. L.; Linford, M. R.; Chidsey, C. E. D. *Langmuir* **2000**, *16*, 5688−5695.
(21) Linford, M. R.; Chidsey, C. E. D. *J. Am. Chem. Soc.* **1993**, *115*, 12631−12632.
(22) Linford, M. R.; Fenter, P.; Eisenberger, P. M.; Chidsey, C. E. D. *J. Am. Chem. Soc.* **1995**, *117*, 3145−3155.
(23) Sieval, A. B.; Demirel, A. L.; Nissink, J. W. M.; Linford, M. R.; van der Mass, J. H.; de Jeu, W. H.; Zuilhof, H.; Sudholter, E. J. R. *Langmuir* **1998**, *14*, 1759−1768.
(24) Sung, M. M.; Kluth, G. J.; Yauw, O. W.; Maboudian, R. *Langmuir* **1997**, *13*, 6164−6168.
(25) Zazzera, L. A.; Evans, J. F.; Deruelle, M.; Tirrell, M.; Kessel, C. R.; McKeown, P. *J. Electrochem. Soc.* **1997**, *144*, 2184−2189.
(26) Zhu, X. Y.; Mulder, J. A.; Bergerson, W. F. *Langmuir* **1999**, *15*, 8147−8154.
(27) Royea, W. J.; Juang, A.; Lewis, N. S. *Appl. Phys. Lett.* **2000**, *77*, 1988−1990.
(28) Bansal, A.; Lewis, N. S. *J. Phys. Chem. B* **1998**, *102*, 1067−1070.
(29) Bansal, A.; Lewis, N. S. *J. Phys. Chem. B* **1998**, *102*, 4058−4060.
(30) Zhu, X. Y.; Jun, Y.; Staarup, D. R.; Major, R. C.; Danielson, S.; Boiadjiev, V.; Gladfelter, W. L.; Bunker, B. C.; Guo, A. *Langmuir* **2001**, *17*, 7798−7803.
(31) Yu, H. Z.; Morin, S.; Wayner, D. D. M.; Allongue, P.; de Villeneuve, C. H. *J. Phys. Chem. B* **2000**, *104*, 11157−11161.
(32) Gu, Y.; Lin, Z.; Butera, R. A.; Smentkowski, V. S.; Waldeck, D. H. *Langmuir* **1995**, *11*, 1849−1851.
(33) Cohen, R.; Kronik, L.; Shanzer, A.; Cahen, D.; Liu, A.; Rosenwaks, Y.; Lorenz, J. K.; Ellis, A. B. *J. Am. Chem. Soc.* **1999**, *121*, 10545−10553.
(34) Sturzenegger, M.; Lewis, N. S. *J. Am. Chem. Soc.* **1996**, *118*, 3045−3046.
(35) Sturzenegger, M.; Prokopuk, N.; Kenyon, C. N.; Royea, W. J.; Lewis, N. S. *J. Phys. Chem. B* **1999**, *103*, 10838−10849.
(36) Sheen, C. W.; Shi, J.-X.; Martensson, J.; Parikh, A. N.; Allara, D. L. *J. Am. Chem. Soc.* **1992**, *114*, 1514−1515.
(37) Hendrickson, D. H.; Sohn, Y. S.; Gray, H. B. *Inorg. Chem.* **1971**, *10*, 1559−1563.
(38) Pomykal, K. E.; Fajardo, A. M.; Lewis, N. S. *J. Phys. Chem.* **1996**, *100*, 3652−3664.
(39) Aspnes, D. E.; Studna, A. A. *Appl. Phys. Lett.* **1981**, *39*, 316−318.
(40) Fajardo, A. M.; Lewis, N. S. *J. Phys. Chem. B* **1997**, *101*, 11136−11151.
(41) Lewis, N. S. *Annu. Rev. Phys. Chem.* **1991**, *42*, 543−580.
(42) Morrison, S. R. *Electrochemistry at Semiconductor and Oxidized Metal Electrodes*; Plenum: New York, 1980.
(43) Chazalviel, J.-N. *Electrochim. Acta* **1988**, *33*, 461−476.
(44) Fahrenbruch, A. L.; Bube, R. H. *Fundamentals of Solar Cells: Photovoltaic Solar Energy Conversion*; Academic: New York, 1983.
(45) Lewis, N. S. *J. Phys. Chem. B* **1998**, *102*, 4843−4855.
(46) Bard, A. J.; Faulkner, L. R. *Electrochemical Methods: Fundamentals and Applications*; Wiley: New York, 1980.
(47) Pomykal, K. E.; Lewis, N. S. *J. Phys. Chem. B* **1997**, *101*, 2476−2484.
(48) Cheng, J.; Robinson, D. B.; Cicero, R. L.; Eberspacher, T.; Barrelet, C. J.; Chidsey, C. E. D. *J. Phys. Chem. B* **2001**, *105*, 10900−10904.
(49) Koval, C. A.; Austermann, R. L. *J. Electrochem. Soc.* **1985**, *132*, 2656−2662.
(50) Bard, A. J.; Bocarsly, A. B.; Fan, F.-R. F.; Walton, E. G.; Wrighton, M. S. *J. Am. Chem. Soc.* **1980**, *102*, 3671−3677.
(51) Spool, A. M.; Daube, K. A.; Mallouk, T. E.; Belmont, J. A.; Wrighton, M. S. *J. Am. Chem. Soc.* **1986**, *108*, 3155−3157.
(52) Bonifazi, D.; Salomon, A.; Enger, O.; Diederich, F.; Cahen, D. *Adv. Mater.* **2002**, *14*, 802−805.
(53) Ashkenasy, G.; Cahen, D.; Cohen, R.; Shanzer, A.; Vilan, A. *Acc. Chem. Res.* **2002**, *35*, 121−128.
(54) Wu, D. G.; Ghabboun, J.; Martin, J. M. L.; Cahen, D. *J. Phys. Chem. B* **2001**, *105*, 12011−12018.
(55) Selzer, Y.; Cahen, D. *Adv. Mater.* **2001**, *13*, 508−511.
(56) Gerischer, H.; Kolb, D. M.; Sass, J. K. *Adv. Phys.* **1978**, *27*, 437−498.
(57) Cooper, G.; Turner, J. A.; Nozik, A. J. *J. Electrochem. Soc.* **1982**, *129*, 1973−1977.
(58) Möllers, F.; Memming, R. *Ber. Bunsen−Ges. Phys. Chem.* **1972**, *76*, 469−475.
(59) Desilvestro, J.; Grätzel, M. *J. Electrochem. Soc.* **1986**, *133*, 331−336.
(60) Fajardo, A. M.; Lewis, N. S. *Science* **1996**, *274*, 969−972.
(61) Royea, W. J.; Fajardo, A. M.; Lewis, N. S. *J. Phys. Chem. B* **1997**, *101*, 11152−11159.
(62) Horrocks, B. R.; Mirkin, M. V.; Bard, A. J. *J. Phys. Chem.* **1994**, *98*, 9106−9114.
(63) Marcus, R. A. *J. Phys. Chem.* **1991**, *95*, 2010−2013.
(64) Cave, R. J.; Newton, M. D. *Chem. Phys. Lett.* **1966**, *249*, 15−19.
(65) (a) Smalley, J. F.; Feldberg, S. W.; Chidsey, C. E. D.; Linford, M. R.; Newton, M. D.; Liu, Y. P. *J. Phys. Chem.* **1995**, *99*, 13141−13149. (b) Sikes, H. D.; Smalley, J. F.; Dudek, S. P.; Cook, A. R.; Newton, M. D.; Chidsey, C. E. D.; Feldberg, S. W. *Science* **2001**, *291*, 1519−1523.
(66) Van der Auweraer, M.; Biesmans, G.; Verschurer, B.; De Schryver, F. C.; Willig, F. *Langmuir* **1987**, *3*, 992−1000.
(67) Nielson, R. M.; McManis, G. E.; Safford, L. K.; Weaver, M. J. *J. Phys. Chem.* **1989**, *93*, 2152−2157.